ELSEVIER

Journal of Nuclear Materials 274 (1999) 167–173

journal of nuclear materials

www.elsevier.nl/locate/jnucmat

Pulse irradiation tests of rock-like oxide fuel

K. Okonogi, T. Nakamura *, M. Yoshinaga, K. Ishijima, H. Akie, H. Takano

Department of Reactor Safety Research, Japan Atomic Energy Research Institute, Tokai-mura, Ibaraki-ken 319-1195, Japan

Abstract

Pulse irradiation tests of special oxide fuel designed for plutonium disposal, called rock-like oxide (ROX), have been conducted in the Nuclear Safety Research Reactor (NSRR) to investigate the transient behavior of ROX fuel under reactivity initiated accident (RIA) conditions. An uranium free ROX, $(Zr,Y)O_2$–$MgAl_2O_4$–PuO_2, is proposed for once-through use of Pu in light water reactors. However, because of smaller negative Doppler and void reactivity coefficients in the ROX fuel, higher peak fuel enthalpies are expected under RIAs than for UO_2 fuel. Thus, the tests of simulated ROX, in which Pu was replaced by U for easier realization, were conducted to a peak fuel enthalpy of 0.96 kJ g^{-1} (230 cal g^{-1}), which is above current Japanese safety limits for UO_2. The transient behavior of the simulated ROX fuel was quite different from that of UO_2, because of its different thermo-physical properties. Fuel failure was associated with fuel melting at peak fuel enthalpies of 1.63 kJ g^{-1} (390 cal g^{-1}) to 2.22 kJ g^{-1} (530 cal g^{-1}). Significant mechanical energy generation, the reason for the limit, however, was not observed.

1. Introduction

On the disposal use of plutonium derived from nuclear weapons or reactors, rock-like oxide (ROX) fuels have been proposed from the viewpoints of proliferation resistivity environmental safety and economy [1–5]. To provide a database for the transient behavior in light water reactors, the behavior of ROX fuel during reactivity initiated accident (RIA) conditions is being studied in the Nuclear Safety Research Reactor (NSRR) at Japan Atomic Energy Research Institute (JAERI). Three pulse irradiation tests of fresh ROX fuel rods have been performed. The objectives of this study are; (1) to understand the fundamental behavior of ROX fuel under RIA conditions, (2) to evaluate the thresholds in terms of the peak fuel enthalpies, modes, and consequences of fuel rod failure. The pulse irradiation was performed in a container-type capsule under a stagnant water cooling condition at atmospheric pressure and ambient temperature. Simulation calculations by FRAP-T6 code were also conducted to estimate the fuel temperature, fuel melt fraction, etc., which could not be measured in the tests.

This paper presents findings obtained from the experimental results of the pulse irradiation tests of ROX fuel, post-irradiation examinations (PIEs), and FRAP-T6 calculations.

2. Experimental procedure

The NSRR is a 'TRIGA-Annular Core Pulse Reactor (ACPR)', utilizing uranium–zirconium hydride (U–ZrH) fuel–moderator elements. The reactor has a dry experimental cavity of 22 cm in inner diameter penetrating the core center. The configuration of the NSRR is illustrated in Fig. 1. The test fuel rod contained in an experimental capsule, shown in Fig. 2, is installed in the experimental cavity and exposed to a high pulsed neutron flux simulating RIA conditions. The capsule is a sealed container of about 200 mm in outer diameter and about 1230 mm in height. A maximum reactivity insertion of 3.36% Δk ($4.6) from zero power is allowed to produce peak reactor power of 21,000 MW, reactor energy release of 108 MW, the full width at half maximum of about 4.4 ms. The pulsing power traces in 3.36% Δk ($4.6) test are illustrated in Fig. 3. Specifications of ROX fuel used in the pulse tests are shown in Table 1. The ROX fuel pellet contains 25.4 mol% of UO_2, 26.8 mol% of yttria stabilized zirconia (YSZ) and 47.8 mol%

* Corresponding author: Fax: +81-29 282 6160; e-mail take@nsrr.tokai.jaeri.go.jp

0022-3115/99/$ – see front matter
PII: S0022-3115(99)00064-1

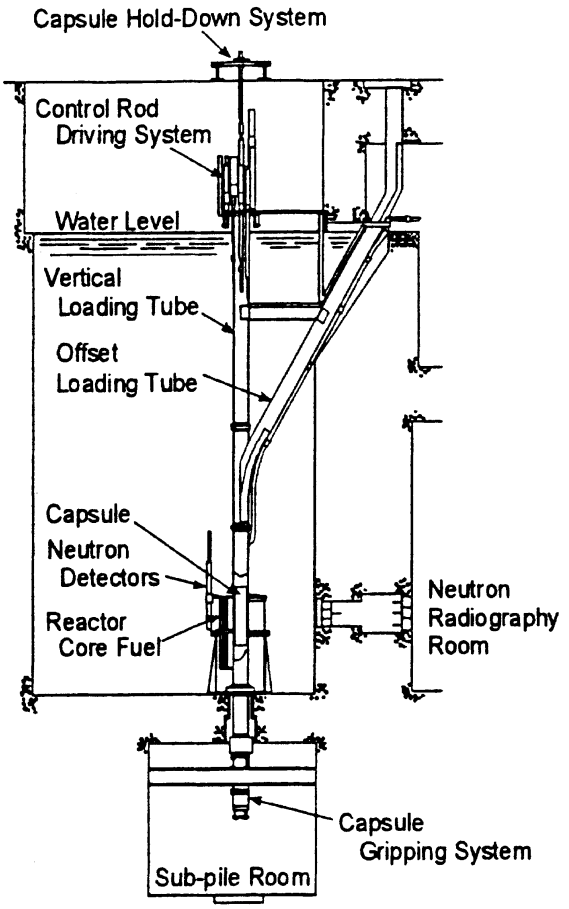

Fig. 1. Configuration of the NSSR.

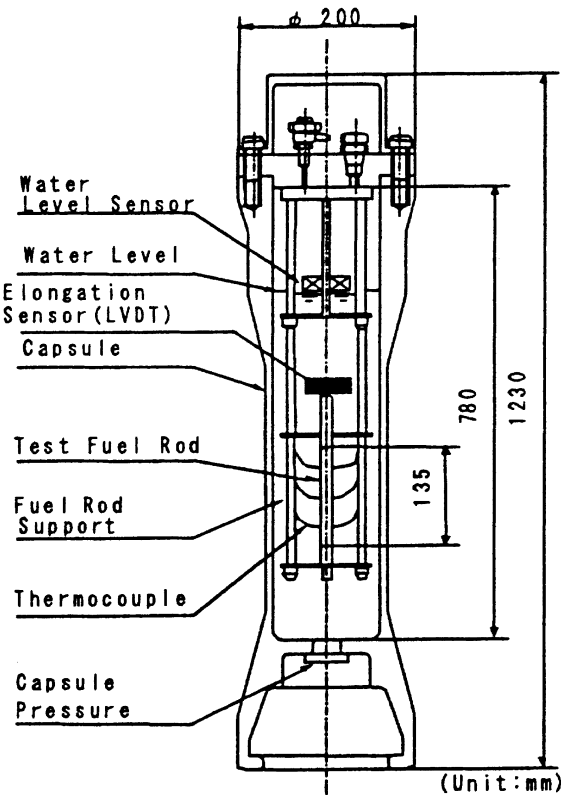

Fig. 2. Experimental capsule of the ROX fuel rod for pulse irradiation in the NSSR.

of spinel ($MgAl_2O_4$). Spinel is added to have larger thermal conductivity and U is used as Pu simulation in the tests. Uranium was enriched to about 20% in U-235. Spinel and YSZ powders were mixed with UO_2 powders, pelletized and sintered at around 2020 K in reducing gas. The compound was in thermodynamical equilibrium and the porosity measured was below around 10%. Measured and estimated thermo-physical properties of the ROX fuel are shown in Table 2 [6,7]. The ROX fuel has lower density (1/2 of UO_2), larger specific heat (2/1 of UO_2), and lower melting temperature (~2200 K). The test fuel rods consisted of a ROX pellet stack about 135 mm long with 14 pellets in the middle surrounded by the Zry-4 cladding, with an upper structure and a bottom structure welded to the cladding, making 279 mm long test fuel rod. The primary specifications of the test rods are the current Japanese 17×17 PWR Type-B rod. During a pulse irradiation tests, cladding surface temperature at three elevations, coolant water temperature, capsule internal pressure, pellet–stack/cladding axial elongation, cladding hoop strain and water column

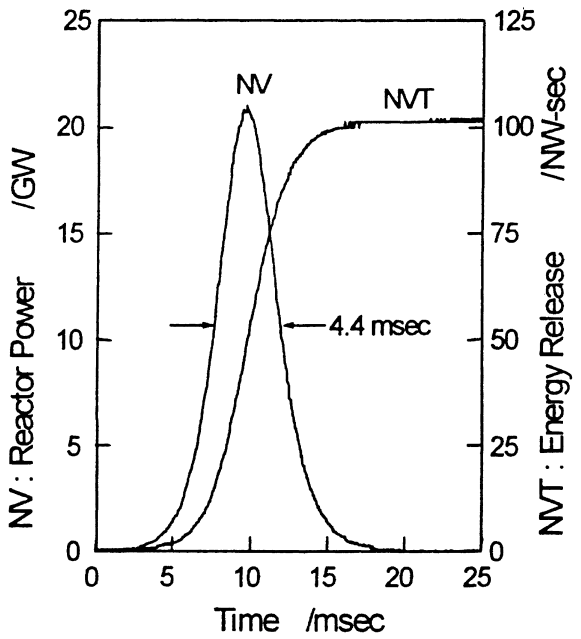

Fig. 3. Reactor power history in the pulse irradiation test at 3.36% Δk (\$4.6).

Table 1
Specifications of ROX fuel rod used in the pulse irradiation tests

Pellet	
Material	UO_2:YSZ:$MgAl_2O_4$
Composition (mol%)	25.4:26.8:47.8
	(YSZ = ZrO_2:Y_2O_3 = 0.812:0.188)
Diameter (mm)	8.05
Length (mm)	9
Enrichment	20% U-235
Cladding	
Material	Zry-4
Outer diameter (mm)	9.5
Wall thickness (mm)	0.64
Element	
Overall length (mm)	279
Fuel stack length (mm)	135
P/C-gap (μm)	85
Filled gas	He at 0.1 MPa

Table 2
Primary thermo-physical properties of ROX and fresh UO_2 fuel

Items	ROX	Fresh UO_2
Pellet density (g cm^{-3})	6	10
Specific heat	0.7 (770 K)	0.3 (770 K)
(J g^{-1} K^{-1})	0.8 (1270 K)	0.3 (1270 K)
Melting temp. (K)	2200	3110
Thermal conductivity	4.3 (770 K)	4.4 (770 K)
(W m^{-1} K^{-1})	3.0 (1270 K)	3.0 (1270 K)
Coefficient of linear thermal expansion (K^{-1})	1.0×10^{-6}	1.2×10^{-6}

movement to trace the transient behavior is measured. The test rod contained in the capsule was irradiated by natural pulse operation at reactivity insertions of 1.97% Δk ($2.7), 2.74% Δk ($3.75) and 3.29% Δk ($4.5). The peak fuel enthalpies were 1.00 kJ g^{-1} (240 cal g^{-1}), 1.63 kJ g^{-1} (390 cal g^{-1}), and 2.22 kJ g^{-1} (530 cal g^{-1}), respectively. The pulse irradiation conditions are summarized in Table 3.

3. Experimental and analytical results

3.1. Fuel rod failure

The appearance of the test rods irradiated in the three tests is shown in Fig. 4. The test fuel rod irradiated at a peak fuel enthalpy of 1.00 kJ g^{-1} in Test 943-1, showed partial oxidation of the cladding surface in the pellet stack region. The one in Test 943-2, did not cause the fuel rod failure though the complete oxidation, slight bulge and bow of the cladding were observed. Cladding

Table 3
Pulse irradiation conditions of the ROX fuel tests

Test no.		943-1	943-2	943-3
Inserted reactivity	(% Δk)	1.97	2.74	3.29
Energy deposition	(kJ g^{-1})	1.42	2.39	2.60
	(cal g^{-1})	(340)	(570)	(620)
Peak fuel enthalpy	(kJ g^{-1})	1.00	1.63	2.22
	(cal g^{-1})	(240)	(390)	(530)

failure occurred in the third Test 943-3 at the peak fuel enthalpy of 2.22 kJ g^{-1}. The cladding did not show the extended embrittlement due to heavy oxidation or thinning of molten cladding, which caused cladding failure of UO_2 fuel rod. The cladding rupture opening was located in the lower part of the fuel stack and considerable amount of the fragmented fuel (about 70%) was dispersed into the water. However, the pressure spike was not observed and the water column movement sensor indicated minor vibration, suggesting that the mechanical energy generation due to molten-fuel/water interaction was not significant in this test.

3.2. Cladding surface temperature

Fig. 5 shows the transient histories of the cladding surface temperature measured during the pulse irradiation Tests 943-1–943-3. The thermocouple attached to the cladding at midheight of the fuel stack in Test 943-1 showed a temperature increase up to about 870 K. The local oxidation of the post pulse cladding and this thermocouple data suggest that departure from nucleate boiling (DNB) occurred locally in this test. In the Test 943-3, the cladding temperature reached about 1770 K which is lower than its melting point (~2120 K), and dropped rapidly to about 1070 K due to decrease of heat capacity by fuel dispersion.

3.3. Fuel rod deformation

Fig. 6 shows the transient histories of the pellet stack and the cladding axial elongation in the second Test 943-2. Cladding peak elongation was 0.8 mm (0.6% of the initial stack length) and 4.2 mm (3.1%) which suggested pellet cladding mechanical interaction (PCMI). Fig. 7 shows the profile of cladding residual hoop strain measured by the post test examination. It should be noted that the test fuel did not fail in Test 943-2 with 1.5% of residual strain at maximum. The Test 943-3 cladding bulging was measured at 4% of diameter around the cladding rupture opening.

3.4. Microstructure

The cross-sectional views of the three test rods are shown in Fig. 8. In the first Test 943-1, many small

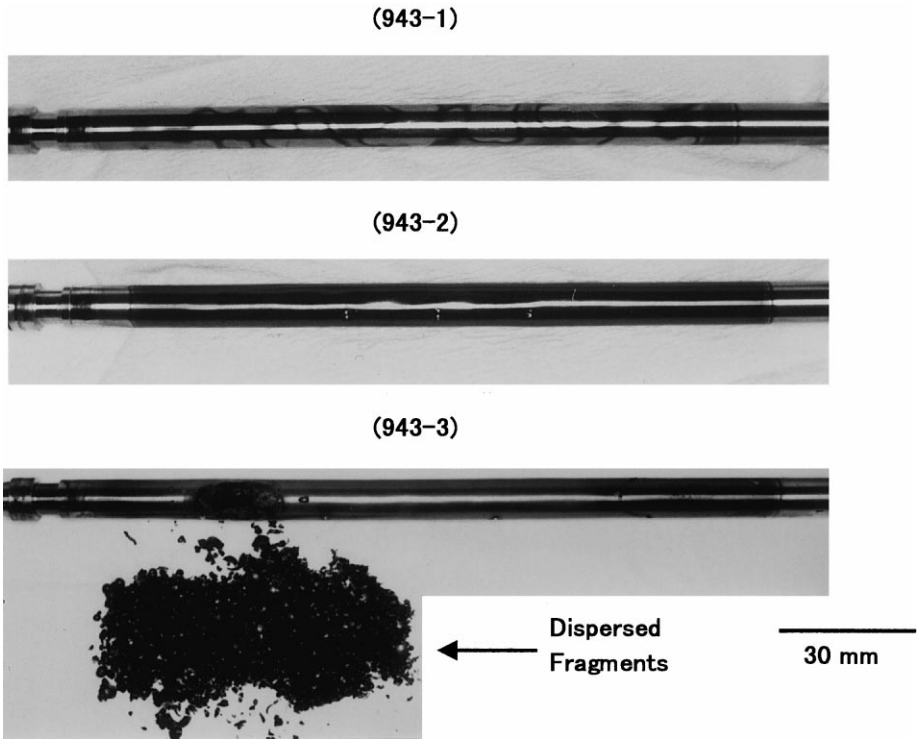

Fig. 4. The appearance of the test rods irradiated in the pulse Tests 943-1–943-3.

radial cracks are seen mostly in the outer region of the fuel, generated by the pulse irradiation, while the micro-structure did not change. As the peak fuel enthalpy increased in the second Test 943-2, the fuel became very porous, a central void was formed, and the micro-structure changed due to the fuel melting. In the third Test 943-3, at the peak fuel enthalpy of 2.22 kJ g^{-1}, most of the fuel appears to have melted and a large amount of the pellets were ejected. A considerable pellet/cladding chemical interaction (PCCI) layer was observed, which likely contributed to the cladding burst.

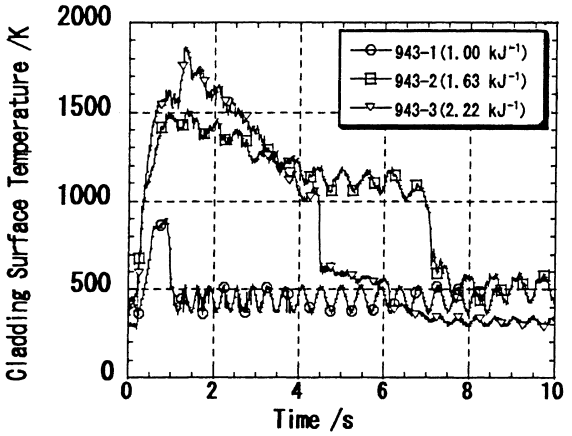

Fig. 5. Transient histories of the cladding surface temperature at midheight of fuel stack measured during the pulse irradiation Tests 943-1–943-3.

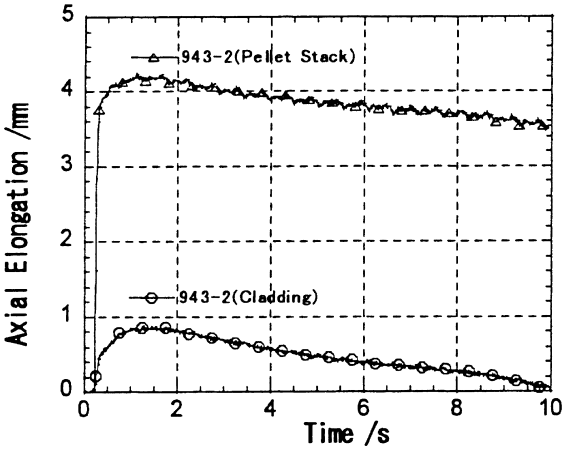

Fig. 6. Transient histories of the pellet and cladding axial elongation in Test 943-2.

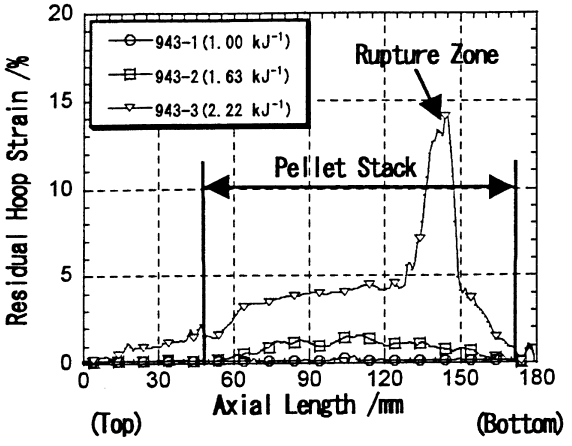

Fig. 7. Profile of cladding residual hoop strain measured by the post-test examination.

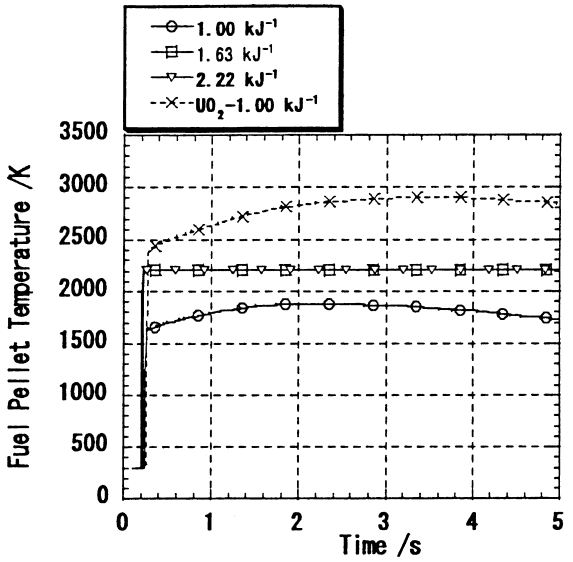

Fig. 9. Fuel pellet temperature histories calculated by the FRAP-T6.

3.5. FRAP-T6 analysis

The fuel rod behavior during the pulse irradiation in the NSRR was simulated with the FRAP-T6 code [8], which was developed for the thermal and mechanical analysis of the transient behavior of $U(Pu)O_2$ fuel rods, and was modified for the NSRR tests [9,10]. The thermo-physical properties of ROX fuel were installed in FRAP-T6 for the ROX test simulation to estimate the fuel temperature, which was not directly measured in the in-pile test. For reference to a comparison with fresh UO_2 fuel behavior, the simulation calculation of UO_2 fuel was also executed with the condition of a

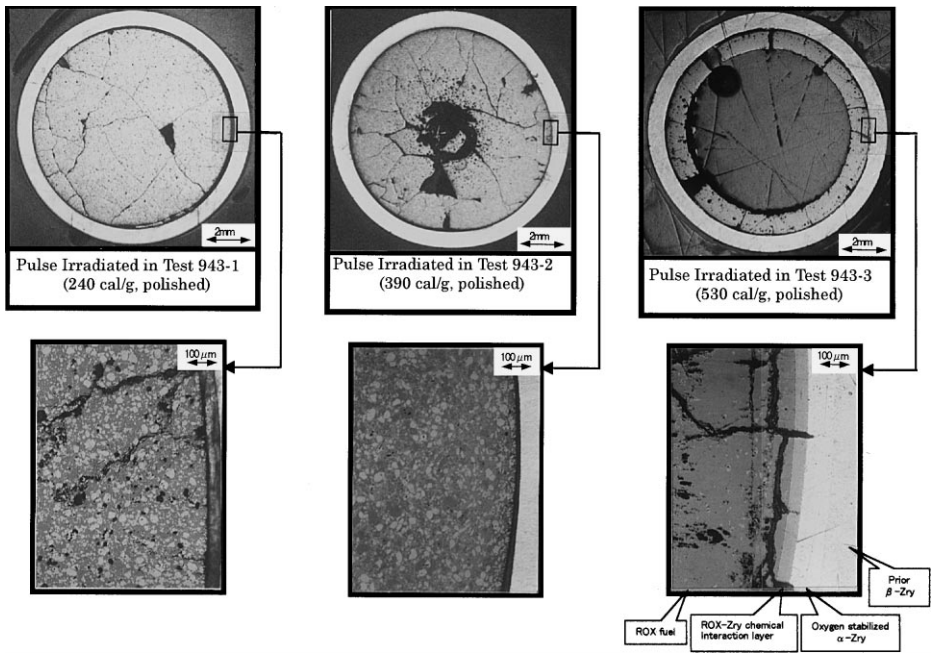

Fig. 8. Cross-sections of the ROX fuel for the pulse tests. It shows central void form due to the fuel melting in Test 943-2 and PCCI in Test 943-3.

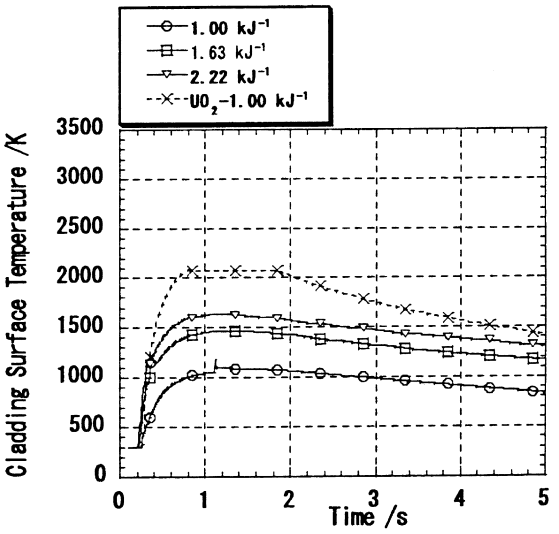

Fig. 10. Cladding surface temperature histories calculated by the FRAP-T6.

peak fuel enthalpy at 1.00 kJ g^{-1}. Figs. 9 and 10 illustrate the fuel pellet and the cladding surface temperature histories calculated by the FRAP-T6. In the ROX fuel test at 1.00 kJ g^{-1}, peak fuel temperature is estimated to have been about 1870 K, which increased the cladding temperature to about 1020 K at the peak. In the ROX fuel test at 1.63 kJ g^{-1}, the fuel temperature is expected to reach its melting point of 2200 K, while the cladding temperature remained about 1470 K, far below its melting point of 2120 K. In this simulation, about 15% of the ROX fuel is predicted to have reached the liquid phase. At the higher fuel enthalpy of 2.22 kJ g^{-1}, the ROX fuel is predicted to be more than 50% molten, though the cladding temperature remains lower than its melting point (~2120 K). On the other hand, in the fresh UO_2 fuel test at 1.00 kJ g^{-1}, the cladding temperature is predicted to have reached its melting point of 2120 K, causing cladding failure due to extensive oxidation embrittlement and thinning by relocation of molten cladding.

FRAP-T6 simulation of the tests shows reasonable agreement with the test results, suggesting that the models for UO_2 are applicable to the ROX fuel.

4. Summary and discussion

Transient behavior of ROX fuel under RIA conditions is compared with that of UO_2 fuel in Table 4. At the same fuel enthalpy, the ROX fuel and its cladding temperature is lower than those of UO_2 fuel rod due to larger specific heat of ROX fuel, resulting in DNB threshold enthalpy to be about 1.00 kJ g^{-1} (the one of UO_2 is 0.46 kJ g^{-1} [11]). Failure of UO_2 fuel rods occurs due to the extended cladding embrittlement by heavy oxidation and thinning as a consequence of cladding melting at a peak fuel enthalpy of 0.89 kJ g^{-1} [11]. On the other hand, the ROX fuel rod did not fail at the peak fuel enthalpy of 1.63 kJ g^{-1}, even though partial fuel melting (~15%) was observed. The lower melting temperature of the ROX (~2200 K) compared to UO_2 (~3110 K) kept the cladding temperature lower than its melting point and prevented thermal failure of the cladding which occurs at peak fuel enthalpies above 0.89 kJ g^{-1} in UO_2 fuel rod. ROX fuel failure occurred at the peak fuel enthalpy of 2.22 kJ g^{-1}. In spite of the cladding rupture and fuel dispersion of about 70%, mechanical energy generation due to molten-fuel/water interaction was not observed. These pulse irradiation tests indicated that the ROX fuel behavior and its failure mechanisms under RIA conditions were quite different from those of UO_2 and the safety limits could be higher for the ROX fuel. However,

Table 4
Comparison of fresh ROX and UO_2 fuel behavior under RIA conditions

Peak fuel enthalpy kJ g^{-1}(cal g^{-1})	Fresh UO_2 fuel rod		Fresh ROX fuel rod		Transient behavior for fuel rod
	Peak clad. temp. (K)	Peak pellet temp. (K)	Peak clad. temp. (K)	Peak pellet temp. (K)	
0.46–0.50(110–120)	370–970	1470			UO_2 DNB threshold (UO_2 cladding oxidation)
0.89(212)	2120	2770			UO_2 failure threshold (UO_2 cladding brittleness)
1.00(240)			870	~1770	ROX DNB threshold (ROX cladding oxidation)
1.17(280)	>2120	3110			UO_2 pellet partial melting (UO_2 cladding melting)
1.36(325)	>2120	3110			UO_2 mechanical energy generation
1.63(390)			1470	~2200	ROX pellet partial melting (pellet melt fraction (~15%)
2.22(530)			1770	~2200	ROX failure without mechanical energy generation (pellet melt fraction (~55%)

the failure condition could be different for irradiated ROX fuel due to fission gases accumulated in the fuel. The fission gas pressure released by fuel melting could cause greater fuel dispersion, resulting in significant mechanical energy generation for irradiated fuel.

5. Conclusions

The ROX fuel behavior under the simulated RIA conditions beyond the current safety limit was studied in the NSRR pulse irradiation tests. The short fuel segments with YSZ–$MgAl_2O_4$–UO_2 fuel pellets in the 17×17 PWR type design were subjected to the simulated RIA conditions at peak fuel enthalpies of 1.00, 1.63 and 2.22 kJ g^{-1}. Cladding rupture and considerable fuel dispersion occurred at the peak fuel enthalpy of 2.22 kJ g^{-1} (fuel melt fraction ~55%). These pulse irradiation tests indicated that the ROX fuel behavior and its failure mechanisms under RIA conditions were quite different from those of UO_2 and the safety limits could be higher for the ROX fuel. This result, however, suggested that ROX fuel rod failure could occur at lower enthalpies for irradiated ROX fuel because fission gas release could cause higher rod pressure.

Acknowledgements

The authors would like to acknowledge and express their appreciation for the time and effort devoted by numerous engineers and technicians in the Reactivity Accident Research Laboratory, NSRR Operation Division and PROFIT team of JAERI.

References

[1] C. Lombardi, A. Mazzola, F. Vettraino, Plutonium annihilation in PWRs via non-fertile inert matrices, in: Proc. Int. Conf. On Evaluation of Emerging Nuclear Fuel Cycle Systems (GLOBAL'95), Versailles, France, vol. 2, 11–14 September 1995, p. 1374.
[2] J.M. Paratte, R. Chawla, Ann. Nucl. Energy 22 (1995) 471.
[3] H. Akie, T. Muromura, H. Takano, S. Matsuura, Nucl. Technol. 107 (1994) 182.
[4] H. Akie, H. Takano, T. Muromura, N. Nitani, A new idea of excess plutonium once-through burning in light water reactor, in: Proc. Int. Symp. Global Environment and Nuclear Energy Systems, Susono, Japan, 24–27 October 1994, Progress in Nucl. Energy, vol. 29 (Suppl.), p. 345.
[5] H. Akie, Y. Anoda, H. Takano, C. Yamaguchi, Y. Sugo, Plutonium Rock-Like Fuel LWR Nuclear Characteristics and Transient Behavior in Accidents, JAERI-Research 98-009, Japan Atomic Energy Research Institute, 1998 (in Japanese).
[6] N. Nitani, T. Yamashita, T. Ohmichi, T. Muromura, Phase relations and thermophysical properties of plutonium rock-like fuels for LWR use, in: Proc. 10th Pacific Basin Nucl. Conf. (10-PBNC), Kobe, Japan, vol. 2, 20–25 October 1996, p. 1114.
[7] T. Matsuda, S. Kobayashi, N. Shirasu, T. Yamashita, T. Ohmichi, T. Muromura, Thermal expansion and thermal conductivity of rock-like fuel, JAERI-Research 97-083, Japan Atomic Energy Research Institute, 1997 (in Japanese).
[8] L.J. Siefken, C.M. Allison, M.P. Bohn, S.O. Peck, FRAP-T6: A computer code for the transient analysis of oxide fuel rods, NUREG/CR-2148, EGG-2104, 1981.
[9] K. Ishijima, T. Nakamura, J. Nucl. Sci. Technol. 33 (3) (1996) 229.
[10] T. Nakamura, H. Sasajima, T. Fuketa, K. Ishijima, J. Nucl. Sci. Technol. 33 (12) (1996) 924.
[11] M. Ishikawa, S. Shiozawa, J. Nucl. Mater. 95 (1980) 1.